Threshold Heat-Flux Reduction by Near-Resonant Energy Transfer

P.W. Terry[1], P.-Y. Li[1], M.J. Pueschel[2,3,4], and G.G. Whelan[1]

[1] *University of Wisconsin-Madison, Madison, Wisconsin 53706, USA*

[2] *Dutch Institute for Fundamental Energy Research,*

5612 AJ Eindhoven, The Netherlands

[3] *Eindhoven University of Technology,*

5600 MB Eindhoven, The Netherlands

[4] *Institute for Fusion Studies, University of Texas at Austin, Austin, Texas 78712, USA*

Abstract

Near-resonant energy transfer to large-scale stable modes is shown to reduce transport above the linear critical gradient, contributing to the onset of transport at higher gradients. This is demonstrated for a threshold fluid theory of ion temperature gradient turbulence based on zonal-flow-catalyzed transfer. The heat flux is suppressed above the critical gradient by resonance in the triplet correlation time, a condition enforced by the wavenumbers of the interaction of the unstable mode, zonal flow, and stable mode.

Turbulence-driven transport arises from the density and temperature gradients of confined plasmas, and has long impeded the realization of fusion power [1]. While it has been possible in some cases to improve confinement without thoroughly understanding the physics of the turbulence that limits it, for example with sheared equilibrium flows [2], fully understanding turbulence could open new strategies for improving confinement, including transport control through externally manipulated barriers [3, 4] and 3D field optimization [5]. Much effort relating to turbulence has centered on identifying and understanding its driving instabilities. Beyond the drive, one may treat linear growth rates as a proxy for turbulence levels and turbulent fluxes, yielding reduced transport models and control strategies based on linear drive physics [6–8].

One notable situation where transport and instability growth rate have distinct behaviors is the critical-gradient upshift of the heat flux of ion temperature gradient (ITG) turbulence. A well known but poorly understood feature first noted in gyrokinetic simulations, this phenomenon, which is often referred to as the Dimits shift, is seen as the onset of transport at a noticeably higher driving gradient than that of linear instability [9]. This critical-gradient upshift is of interest not just because the onset of transport at a higher driving gradient represents a form of transport reduction, but because it exposes a crucial piece of nonlinear saturation physics relevant to a variety of issues [5, 10].

Identifying the mechanism of the critical-gradient upshift has proved elusive. Transport suppression by the shearing of zonal flows is often invoked [11–13]. Zonal flows are the $k_y = 0$ component of the turbulent flow; the rate at which they shear eddies to a flow-wise correlation length is referred to as the E×B shearing rate [2]. In the original observation of the critical-gradient upshift, it was noted that the E×B shearing rate exceeds the growth rate in the region of very low transport [above the linear instability threshold but below the nonlinear critical gradient (NLCG)] [9]. This idea was further developed in the notions of tertiary instability [14] and critical onset of strong nonlinear energy transfer from zonal flows [15], whose coincidence with the NLCG is argued to interfere with zonal flow shearing. We show that this picture is inconsistent with observations in gyrokinetic simulations of ITG turbulence. Recent work exploring finite-amplitude-induced changes in electron drift-wave turbulence from the inhomogeneity of zonal flows expands investigation of the relation between flow and turbulence [16, 17], but is not directly applicable to the ITG threshold.

The principal result of this letter is an analytic theory for the heat flux based on an

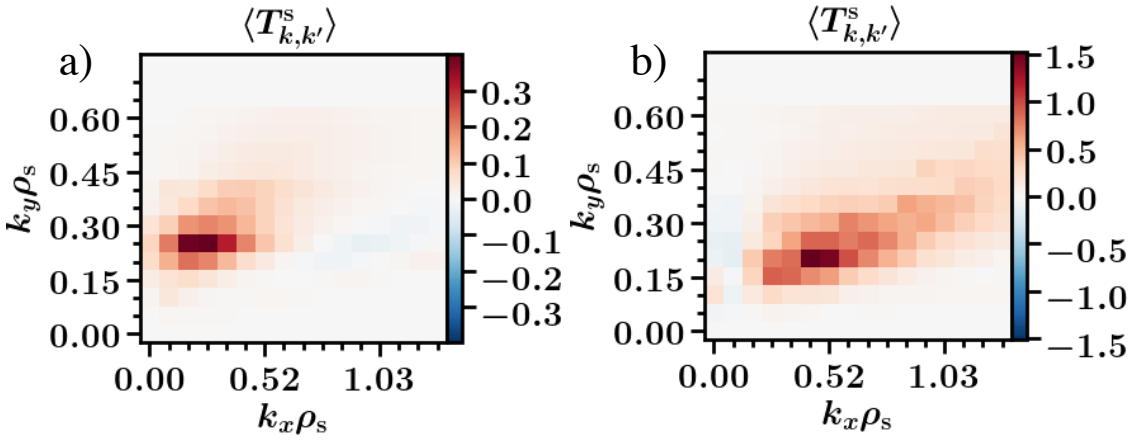

FIG. 1. Rates of spectral energy transfer in gyrokinetic ITG turbulence. In a) $\omega_{T\rm i} = 5.5$, above the linear threshold of 4.75 but below the NLCG of 6.75. In b) $\omega_{T\rm i} = 7.0$.

extension of ITG fluid saturation theory [18] to include the instability threshold. The calculation requires a more rigorous saturation analysis to account for a finite wavenumber range and the partition of energy between eigenmodes. We show that the ion heat flux is weakened above the linear critical gradient by near-resonant energy transfer between the instability, the zonal flow, and a conjugate stable mode. Resonance broadening by eddy damping and mode dispersion from the ion polarization drift expose gradient scalings that cancel in the non-broadened resonance, allowing the flux to rise more sharply at steeper gradients. This mechanism, which captures key aspects of the critical-gradient upshift, has not been considered in prior theories.

The key aspects just mentioned are uncovered in the behavior of nonlinear energy transfer above and below the NLCG in gyrokinetic ITG turbulence, where the critical gradient phenomenon was first observed. Figure 1 shows the time rate of change of energy carried conservatively between spatial scales by turbulence for GENE [19] gyrokinetic flux-tube simulations at Cyclone-Base-Case (CBC) parameters [9] with adiabatic electrons using two values of the temperature gradient $\omega_{T\rm i} = -(R/T_{i0})(dT_{i0}/dx)$, where R is the major radius, T_{i0} (T_{e0}) is the equilibrium ion (electron) temperature, and x is the radial coordinate. Linear instability occurs above $\omega_{T\rm i} = 4.75$ and the NLCG is $\omega_{T\rm i} = 6.75$. In Fig. 1a) for $\omega_{T\rm i} = 5.5$, colors indicate the time averaged energy transfer rate to a sequence of stable modes at successively higher k_x from the interaction of streamers $(0,\, k_y)$ with a single zonal flow $(0.086,\, 0)$. Here k_x is the radial wavenumber and k_y is the wavenumber perpendicular to k_x and

the magnetic field. Both are normalized to the ion sound gyroradius ρ_s. Unstable modes at higher k_x receive less energy by an order of magnitude. In Fig. 1b) for $\omega_{T\mathrm{i}} = 7.0$, the interacting zonal flow is (0.04, 0). A second set of measurements of transfer from streamers to all coupled wavenumbers indicates that for both gradient values, coupling with a zonal flow dominates. In comparing a) and b), energy transfer is larger above the NLCG, consistent with higher turbulence levels, and is therefore able to push to somewhat higher k_x. The energy transfer process appears to be qualitatively the same, and is consistent with transfer from unstable modes to stable modes through the zonal flow. This is referred to as the zonal-flow-catalyzed energy transfer channel.

Figure 2 shows the ratio of the E×B shearing rate to the linear growth rate as a function of $\omega_{T\mathrm{i}}$. The NLCG is shown as the dashed line. E×B shearing by the zonal flow is important below the NLCG because the ratio is greater than unity, as noted in Ref. [9]. However, as the turbulent amplitudes rise above the NLCG the ratio becomes larger. This is inconsistent with the notion that a breakdown of shear suppression causes the rising heat flux above the NLCG. It is consistent with the relatively stronger zonal-flow-catalyzed energy transfer channel evident in Fig. 1b), while indicating that the zonal flow nonetheless remains the dominant energy transfer channel below the NLCG. Note that zonal-flow catalyzed energy transfer is a straining process of the zonal flow and thus proportional to the flow shear.

These observations indicate that there is a single saturation process – zonal-flow-catalyzed energy transfer – which is highly efficient just above the linear critical gradient (yielding low fluxes) and less so as gradients increase. ITG saturation theory for zonal-flow-catalyzed transfer [18], when modified to include instability threshold physics, produces precisely this behavior. We start with a simplified gyrokinetic linear instability calculation [20] and adapt it to the nonlinear fluid model. The calculation retains gyrokinetic ions, but treats the grad-B and curvature drifts non-resonantly, expanding the kinetic propagator for large frequency relative to the magnetic frequency. Parallel streaming and ion polarization effects are neglected. Calculating $\tilde{n}_i$ from the ion distribution function, and using quasineutrality with an adiabatic electron density, we obtain the complex mode frequency $\omega = \omega_d \pm \sqrt{\omega_d^2 - (T_{i0}/T_{e0})(2\omega_d\bar{\omega}_{*\eta} - 7\omega_d^2)}$. Here $\omega_d = -k_y\rho_s C_s/R$, $\bar{\omega}_{*\eta} = \omega_*(1+\eta) = -k_y\rho_s C_s(1/L_T + 1/L_n)$, L_T and L_n are ion temperature and density gradient scale lengths, and C_s is the sound speed. Instability requires that $\bar{\omega}_{*\eta}$ exceed a threshold, i.e., $\bar{\omega}_{*\eta} > (\omega_d/2)(7 + T_{e0}/T_{i0})$. For $L_T \ll L_n$ ($\eta \gg 1$) this corresponds to a

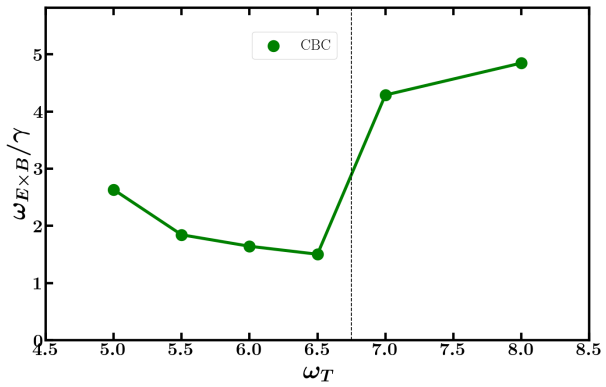

FIG. 2. Ratio of E×B shearing rate to linear growth rate in gyrokinetic ITG turbulence for an $\omega_{T\mathrm{i}}$ scan. The dashed line is the NLCG.

critical gradient given by $1/L_T > 1/L_{Tc} = (1/2R)(7 + T_{e0}/T_{i0})$. Lack of dispersion produces a resonant interaction between the unstable ITG mode, its conjugate pair, and the zonal flow. For resonance the heat flux is essentially zero. It is broadened by ion polarization, leading to a small finite flux.

The reduced nonlinear model to which the linear threshold calculation will be adapted was previously used for saturation well above the threshold [18]. The model [21] reproduces important features of gyrokinetic simulations [15, 22], including the dominance of the zonal-flow-catalyzed energy transfer channel. Its quadratic dispersion relation allows the threshold dispersion to be reproduced with minor changes; it does not have the large number of stable modes of gyrokinetics. The analytic solution involves zonal-flow damping, making it unable to replicate collisionless physics.

The nonlinear model couples ion pressure p and potential ϕ given by $dp_k/dt + Z_{11}p_k + Z_{12}\phi_k = N_p$ and $d\phi_k/dt + Z_{21}p_k + Z_{22}\phi_k = N_\phi$, where Z_{ij} are the linear coupling coefficients defined in Table 1 for the fluid model of Ref. [21] and the modified model that matches the threshold dispersion; the nonlinearities are $N_p = -\sum_{k'} \mathbf{k}' \times \hat{\mathbf{z}} \cdot \mathbf{k}\, \phi_{k'} p_{k''}$ and $N_\phi = (1/2)\sum_{k'} \mathbf{k}' \times \hat{\mathbf{z}} \cdot \mathbf{k}\, (k_\perp'^2 - k_\perp''^2)\phi_{k'}\phi_{k''}$; $\hat{\mathbf{z}}$ is the unit vector along the field, $\mathbf{k} = (k_x, k_y)$, $k_\perp^2 = k_x^2 + k_y^2$, and $k'' \equiv k - k'$ label coupled wavevectors. Flow damping ν and a thermal diffusivity χ have been added as in Ref. [15]. Both the original and modified models include the ion polarization drift, leading to factors $(1 + k_\perp^2)^{-1}$ in Z_{21} and Z_{22}. As in Refs. [15, 21],

Coupling Coefficient	Original Model (Refs. [15, 21])	Threshold Model
Z_{11}	$\chi k_\perp^4$	$\chi k_\perp^4 + i\epsilon k_y(1+\sqrt{8})$
Z_{12}	$ik_y(1+\eta)$	$ik_y(1+\eta)$
Z_{21}	$-2i\epsilon k_y/(1+k_\perp^2)$	$-2i\epsilon k_y/(1+k_\perp^2)$
Z_{22}	$(ik_y+\nu k_\perp^2-2i\epsilon k_y)/(1+k_\perp^2)$	$[ik_y+\nu k_\perp^2-i\epsilon k_y(\sqrt{8}-1)]/(1+k_\perp^2)$

TABLE I. Linear coupling coefficients for two-fluid models of ITG turbulence. The threshold model matches the linear dispersion relation of the kinetic threshold calculation of Ref. [20].

$T_{e0} = T_{i0}$, and the parallel length scale is normalized to L_n, rendering ω_d as $k_y\epsilon \equiv k_y L_n/R$. The threshold model differs from the original primarily by inclusion in the pressure equation of a term $\propto i\omega_d p$. Assuming the extra factor of $k_\perp^2$ makes $\chi k_\perp^2 \ll \nu$, the complex mode frequency of the threshold fluid model is

$$\omega_{1,2} = \frac{\epsilon k_y[2+(1+\sqrt{8})k_\perp^2]+k_y-i\nu k_\perp^2}{2(1+k_\perp^2)} \pm \frac{\sqrt{-8\epsilon k_y^2(1+\eta)(1+k_\perp^2)+\left[\epsilon k_y(2\sqrt{8}+(1+\sqrt{8})k_\perp^2)-k_y+i\nu k_\perp^2\right]^2}}{2(1+k_\perp^2)}, \tag{1}$$

where the subscript 1(2) labels the unstable (stable) branch, selected by + (–) in ±. With $k_y(1+\eta) = \omega_{*\eta} \sim 1$, $\epsilon k_y = \omega_d \sim 1$, and taking k_y, $k_\perp^2 \ll 1$, this expression exactly matches the threshold frequency for $T_{e0} = T_{i0}$. Hereafter we use the threshold fluid model and the notation of Table 1, retaining finite $k_\perp^2$ in Z_{ij} because it broadens the mode coupling resonance.

The ion heat flux is an ensemble average of the product of fluctuations p and ϕ, $Q_i = -\sum_{k'} k'_y \mathrm{Im}\langle \phi_{-k'} p_{k'}\rangle$. We introduce the eigenmode decomposition, $p_{k'} = R'_1\beta'_1 + R'_2\beta'_2$ and $\phi_{k'} = \beta'_1 + \beta'_2$, where R'_j and β'_j are eigenvector components and amplitudes, and quantities with primes are evaluated at k'. The flux is then given by $Q_i = -\sum_{k'} k'_y[\mathrm{Im}R'_1\langle|\beta'_1|^2\rangle + \mathrm{Im}R'_2\langle|\beta'_2|^2\rangle + \mathrm{Im}(R'_1+R'_2)\mathrm{Re}\langle\beta'_1\beta'^*_2\rangle + \mathrm{Re}(R'_1-R'_2)\mathrm{Im}\langle\beta'_1\beta'^*_2\rangle]$. From the eigenfrequencies we obtain $R'_j = [-\omega'_j(1+k'^2_\perp)+k'_y(1+\epsilon(1-\sqrt{8}))-i\nu k'^2_\perp]/2k'_y\epsilon$, where ω'_j is the jth eigenfrequency at k'. Above the linear threshold $\mathrm{Re}(R'_1-R'_2) = 0$ and $\mathrm{Im}(R'_1+R'_2) = -3\nu k'^2_\perp/2k'_y\epsilon$. The ratios of eigenmode amplitudes can be solved from the balances of the saturation theory [2], and reduce to ratios of the linear eigenmode frequencies and nonlinear coupling coefficients. The latter also reduce to functions of eigenmode frequencies.

We evaluate Q_i in terms of the stable fraction $\kappa \equiv |\beta'_2|^2/|\beta'_1|^2$. We can thus write $\beta'_2 = \beta'_1\sqrt{\kappa}\exp(i\theta)$, where θ is the cross phase between β'_1 and β'_2. The cross correla-

tion becomes $\langle\beta_1'^*\beta_2'\rangle = |\beta_1'|^2\kappa^{1/2}\exp(i\theta)$. From the eigenvector components and the above ratios, we find $Q_i = \sum_{k'}(\gamma'/2\epsilon)(1+k_\perp'^2)|\beta_1'|^2(1-\kappa)$, to lowest order in $\nu/k_y'\epsilon$, where $\gamma' = \mathrm{Im}\omega_1'$. To complete the heat flux derivation we obtain the saturation level $|\beta_1'|^2$ from Eq. (A4) of Ref. [18], with coupling coefficients and frequencies supplied from the threshold model. This equation is the steady-state turbulent energy balance evaluated at the zonal wavenumber ($k_y = 0$). We derive here a more rigorous solution than that of Ref. [18]. Because the wavenumber k' is summed over, we change the summation variable from $k-k'$ to k'. This allows the nonlinear coupling coefficients to be grouped as $C_{iFj}^{(k'',k)} + C_{ijF}^{(k'',-k')} = (-1)^{i-1}k_y'[\omega_j'(1+k_\perp'^2) + k_y'(1+\epsilon(1-\sqrt{8})) + i\nu k_\perp'^2]/[2\mathrm{Im}\omega_1''(1+k_\perp''^2)] \equiv C_{ij}''$, where $i \neq j$ is 1 or 2, and ω_j'' is evaluated at k''. In terms of C_{ij}'' the zonal saturation balance can be written $\nu = 4\sum_{k'}\mathrm{Re}\{C_{F21}^{(k,k')}[|\beta_1'|^2(\tau_{21F}C_{21}'' + \tau_{12F}C_{12}''\kappa) + \mathrm{Re}\langle\beta_1'^*\beta_2'\rangle(\tau_{12F}C_{11}'' + \tau_{21F}C_{22}'') + i\mathrm{Im}\langle\beta_1'^*\beta_2'\rangle(\tau_{12F}C_{11}'' - \tau_{21F}C_{22}'')]\}|_{k_y=0}$, where unprimed frequencies are evaluated at k, $\tau_{21F} = (i\hat{\omega}_2'' + i\hat{\omega}_1' - i\hat{\omega}_1^*)^{-1}$ and $\tau_{12F} = (i\hat{\omega}_1'' + i\hat{\omega}_2' - i\hat{\omega}_1^*)^{-1}$ are triplet correlation times for the zonal-flow-catalyzed interaction, $C_{F21}^{(k,k')} = -ik_y'[k_\perp'^2 - (k_\perp - k_\perp')^2]/2$, and $\hat{\omega}_i = \omega_i + \Delta\omega_i$ is the sum of the linear frequency and a nonlinear eddy-damping rate $\Delta\omega_i$. The eddy damping rate describes the decorrelation of a given mode frequency from interactions with other turbulent modes.

As a nonlinear frequency, $\Delta\omega_i$ is proportional to k^2 and the turbulence level [23]. Because $\omega_i \propto k$, nominally $\Delta\omega_i \ll \omega_i$ for $k \ll 1$, allowing eddy damping to be ignored. However, for certain wavenumbers τ_{12F} (or τ_{21F}) is resonant, meaning $\omega_2'' + \omega_1' - \omega_1^* = 0$. In such cases $\Delta\omega_i$ dominates τ_{12F} even for $k \ll 1$ and at low turbulence levels. Resonance is intrinsic to stable-mode saturation by zonal-flow-catalyzed transfer if the ion polarization drift is neglected ($k_\perp^2 \to 0$) and $\nu \to 0$. This is because the three-wave coupling condition $k' + k'' = k$ leads directly to $\omega_2'' + \omega_1' - \omega_1^* \to 0$ when k is the wavenumber of the zonal flow ($k_y = 0$). Note that even with $k_\perp$ finite but small, the contribution of the ion polarization drift to τ_{12F} is $\mathrm{O}(k_\perp^3)$, making it smaller than the contribution of $\Delta\omega_i$.

We obtain an expression for $\Delta\omega_i$ to determine its dependence on η, deriving it from the energy response to an infinitesimal perturbation in the turbulent state [24]:

$$\Delta\omega_i = \sum_{k'} \frac{-2iC_{iFj}^{(k,k')}}{i\hat{\omega}_j'' - i\hat{\omega}_i^* + i\hat{\omega}_i'} \left[C_{ij}''|v_z'|^2 + C_{Fij}^{(k',k)}\left(|\beta_2''|^2 + \langle\beta_1''^*\beta_j''\rangle\right)\right]\Bigg|_{k_y'=0}. \qquad (2)$$

Here $C_{iFj}^{(k,k')} = [-\omega_j''(1+k_\perp''^2) + k_y''(1+\epsilon(1-\sqrt{8})) + i\nu k_\perp''^2]/[(\omega_2-\omega_1)(1+k_\perp^2)]$, and the zonal

flow $v'_z = ik'_x\beta'_1|_{k'_y=0} = ik'_x\phi'|_{k'_y=0}$ enters $\Delta\omega_i$ as part of the turbulent spectrum.

The saturation balance is solved by assuming that all relevant wavenumbers are $\ll 1$. We consider the interactions of a zonal flow at $(-k'_x, 0)$, an unstable streamer at $(0, k'_y)$, and a stable-mode sideband at (k'_x, k'_y). This leads to $|\beta'_1|^2 = \nu\Big[4\mathrm{Re}\big\{C_{F21}^{(k,k')}\big[\tau_{21F}\big(C''_{21} + C''_{22}\sqrt{\kappa}\exp(-i\theta)\big) + \tau_{12F}\big(C''_{12}\kappa + C''_{11}\sqrt{\kappa}\exp(i\theta)\big)\big]\big\}\Big]^{-1}$. A more general expression is obtained from a standard Markovian assumption that $|\beta'_1|^2$ varies more slowly than the other wavenumber-dependent factors in the saturation balance arising from coupling coefficients and τ factors. With this approximation, $|\beta'_1|^2$ is understood as evaluated at a typical unstable wavenumber, and the denominator is summed over k'. Considering the zonal saturation balance for other k_x introduces a sum over k_x. The cross phase θ is obtained from a symmetry of the nonlinearity that leads to the constraint $\sum_j d[\beta'_j\exp(i\omega'_j t)]/dt = 0$. Introducing $\beta'_2 = \beta'_1\sqrt{\kappa}\exp(i\theta)$ as before, the constraint is solved to obtain $\theta = -\alpha + \sin^{-1}[\mathrm{Im}(\omega_1'^* - \omega'_2\kappa)\kappa^{-1/2}|\omega'_2 - \omega_1'^*|^{-1}]$, where α is the complex phase of $\omega'_2 - \omega_1'^*$.

Substituting the Markovianized solution for $|\beta'_1|^2$ into the heat flux, we obtain

$$Q_i = \sum_{k'''} \frac{\gamma(k''')(1+k_\perp'''^2)\nu(1-\kappa)}{4\epsilon\sum_{k_x,k'}(k_\perp'^2 - k_\perp''^2)\mathrm{Re}\Big(ik'_y\Big[\tau_{21F}\big(C''_{21} + C''_{22}\sqrt{\kappa}e^{-i\theta}\big) + \tau_{12F}\big(C''_{12}\kappa + C''_{11}\sqrt{\kappa}e^{i\theta}\big)\Big]\Big)}. \tag{3}$$

The factor $k_\perp'^2 - k_\perp''^2$ has been extracted from $C_{F12}^{(k,k')}$ because it produces along with $\gamma(k''')$ a quasilinear-flux-like factor. The remaining factors, which include the triplet correlation time and coupling coefficients, represent nonlinear contributions to a critical-gradient upshift. There is considerable symmetry in pieces of the denominator, leading to partial cancellations. Moreover, the complex phase of the factors inside the real part is important in the dependence of Q_i on η. Figure 3 shows the dependence of Q_i on η for a case driven by the streamer $(0, 0.25)$ with $\nu = 0.001$, $\kappa = 0.9999$ and two values of ϵ. $\nu = 0.001$ keeps the system close to collisionless, while still balancing nonlinear excitation of the zonal flow. A larger ϵ of 1.25 was chosen to put a threshold η between 2 and 3. The smaller ϵ reduces the threshold while showing qualitatively similar behavior. The theoretical results are plotted alongside numerical solutions of the nonlinear model, showing reasonable agreement. A NLCG is more easily defined from the simulation results than the theory, but the behavior is consistent with the notion of flux reduction close to the threshold. A scan in η for larger collisionality $\nu = 0.0025$ shows very similar behavior.

The behavior of Fig. 3 resides in τ and the coupling coefficients. The former is near-

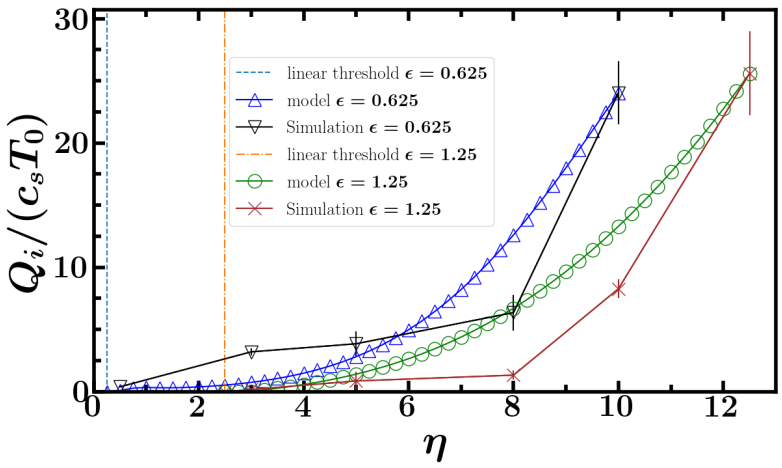

FIG. 3. Heat flux as a function of η for $\epsilon = 0.625$ and $\epsilon = 1.25$: analytic theory (triangles and circles), numerical solution (inverted triangles and crosses).

resonant, maximizing its value for the zonal-flow catalyzed triplet, yielding $\tau = \infty$ and $Q_i = 0$ if $\Delta\omega_i = \nu = k_\perp^2 = 0$. With these quantities finite but small, τ and Q_i are finite; τ decreases and Q_i increases with η, because ω increases with η. The variation of τ and C_{iFj} are shown in Fig. 4. Variation of the latter, which is dominated by the ratio $[\mathrm{Re}(\omega) + i\gamma]/\gamma$, is strongest just above the threshold, where $C_{iFj} \sim \mathrm{Re}(\omega)/\gamma$, and asymptotes to a constant for large η. This variation strongly contributes to reduced Q_i just above the threshold, and to eddy damping. Near the threshold, the first term of Eq. (2) dominates, both because of its proportionality to $|v_Z|^2$ and because C_{iFj} is much larger than C_{F12} for small k. The eddy damping is therefore proportional to C_{iFj}^2, which makes it significant only near threshold. It smooths countering trends in τ arising from the scaling of ω_2'' and ω_1 with η just above threshold, and exposes the matched scalings of these two frequencies once η increases above 5. The stable fraction $\kappa = |\beta_2|^2/|\beta_1|^2$ is governed by the equipartition of energy dissipation rates $\gamma_1|\beta_1|^2 = |\gamma_2||\beta_2|^2$, a property of stable-mode saturation [22]. For a conjugate mode pair, $\kappa = 1$. Collisionality breaks conjugate symmetry, making κ slightly less than unity. The value used in Fig. 3 is consistent with $\gamma_1/|\gamma_2|$ at larger η. Near instability threshold, $\eta - \eta_c < 1$, the saturation characterization $\gamma_1|\beta_1|^2 = |\gamma_2||\beta_2|^2$ becomes unreliable because of branch points in the complex mode frequencies that occur at different values of η due to threshold dependence on $k_\perp^2$. In this region κ is extrapolated from its value at larger η.

This resonance is important in gyrokinetic manifestations of critical-gradient behavior

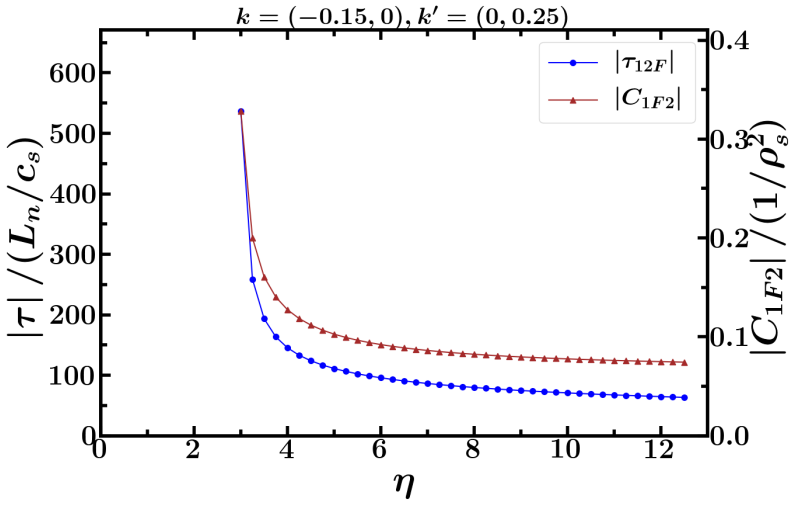

FIG. 4. Variation of triplet correlation times and coupling coefficient C_{1F2} with η.

[25] and in the nonlinear stabilization of ITG turbulence at finite β [26]. (β is the plasma pressure normalized to the magnetic energy of the confining field.) In the latter the flux is very small *below* the linear β threshold and only begins to rise at lower β. This occurs because large τ near threshold makes Q_i very small, while resonance broadening in the form of finite $k_\perp^2$ exposes stronger dependence on β, allowing it to rise more sharply further below the threshold as $\beta \to 0$. This effect has been demonstrated by gyrokinetic modeling of experimental discharges [27]. The unitarity of mechanisms for the critical-gradient upshift and finite-β nonlinear stabilization, combined with the fact that the latter occurs where zonal-flow shearing is weakened by magnetic fluctuations [28], strongly suggests that shear suppression cannot be the mechanism of the critical-gradient upshift.

This letter has demonstrated that the nonlinear energy transfer properties of ITG turbulence, aside from magnitudes, are essentially unchanged above and below the NLCG, with no disabling of E×B shearing. Motivated by these observations, the theoretical and conceptual basis for a new physical explanation of nonlinear critical-gradient upshift behavior has been developed, accounting for three-wave resonance in the dominant saturation mechanism of zonal-flow catalyzed transfer to stable modes.

This work was supported by US Department of Energy Grant DE-FG02-89ER53291.

[1] W. Horton, Rev. Mod. Phys. **71**, 735 (1999).

[2] P.W. Terry, Rev. Mod. Phys. **72**, 109 (2000).

[3] E.J. Strait et al., Phys. Rev. Lett. **75**, 4421 (1995).

[4] D.E. Newman, B.A. Carreras, D. Lopez-Bruna, P.H. Diamond, and V.B. Lebedev, Phys. Plasmas **5**, 938 (1998).

[5] C.C. Hegna, P.W. Terry and B.J. Faber, Phys. Plasmas **25**, 022511 (2018).

[6] R.E. Waltz, G.D. Kerbel, and J. Milovich, Phys. Plasmas **1**, 2229 (1994).

[7] C. Bourdelle, X. Garbet, F. Imbeaux, A. Casati, N. Dubuit, R. Guirlet, and T. Parisot., Phys. Plasmas **14**, 112501 (2007).

[8] H.E. Mynick, N. Pomphrey, and P. Xanthopoulos, Phys. Rev. Lett. **105**, 095004)

[9] A.M. Dimits et al., Phys. Plasmas, **7**, 969 (2000).

[10] P. Mantica et al., Phys. Rev. Lett. **102**, 175002 (2009).

[11] B.N. Rogers, W. Dorland, and M. Kotschenreuther, Phys. Rev. Lett. **85**, 5336 (2000).

[12] K. Miki, Y. Kishimoto, N. Miyato, and J.Q. Li, Phys. Rev. Lett. **99**, 145003 (2007).

[13] S.-I. Itoh and K. Itoh, Nucl. Fusion **56**, 106028 (2016).

[14] F. Rath, A.G. Peeters, R. Buchholz, S.R. Grosshauser, F. Seiferling, and A. Weikl, Phys. Plasmas **25**, 052102 (2018).

[15] C. Holland, P.H.Diamond, S. Champeaux, E. Kim, O. Gurcan, M.N. Rosenbluth, G.R. Tynan, N. Crocker, W. Nevins, and J. Candy, Nucl. Fusion **43**, 761 (2003).

[16] D.A. St-Onge, J. Plasma Phys. **83**, 905830504 (2017).

[17] H. Zhu, Y. Zhou, and I.Y. Dodin, Phys. Rev. Lett. **124**, 055002 (2020).

[18] P.W. Terry, B.J. Faber, C.C. Hegna, V.V. Mirnov, M.J. Pueschel, and G.G. Whelan, Phys. Plasmas **25**, 012308 (2018).

[19] F. Jenko, W. Dorland, M. Kotschenreuther, and B.N. Rogers, Phys. Plasmas **7**, 1904 (2000).

[20] G. Hammett, UCLA Winter School, Center for Multiscale Plasma Dynamics, Los Angeles, CA, Jan. 2007.

[21] W. Horton, D.-I. Choi, and W.M. Tang, Phys. Fluids **24**, 1077 (1981).

[22] P.W. Terry, K.D. Makwana, M.J. Pueschel, D.R. Hatch, F. Jenko, and F. Merz, Phys. Plasmas **21**, 122303 (2014).

[23] P.W. Terry and W. Horton, Phys. Fluids **26**, 106 (1983).

[24] R.H. Kraichnan, J. Fluid Mech. **5**, 497 (1959).

[25] M.J. Pueschel, P.-Y. Li, and P.W. Terry, submitted to PRL.

[26] M.J. Pueschel and F. Jenko, Phys. Plasmas **17**, 062307 (2010).

[27] G.G. Whelan et al., Phys. Plasmas **26**, 082302 (2019).

[28] Z.R. Williams, M.J. Pueschel, P.W. Terry, T. Nishizawa, D.M. Kriete, M.D. Nornberg. J.S. Sarff, G.R. McKee, D. M. Orlov, and S.H. Nogami, Nucl. Fusion **60**, 096004 (2020).